inter.noise
HAMBURG 2016

Active Control of Impact Sound

André V. V. PASSANESI[1]; Wolfgang KROPP[2];

[1,2] Chalmers University of Technology, Sweden

ABSTRACT

Impacts are an important noise source of today's society. From a control standpoint, solutions to problems related to impacts are commonly based on passive methods. In this paper, an active method to control the radiated sound from a sphere impacting a simply supported plate attached to an infinite baffle is proposed. The contact force between sphere and plate is modeled by Hertzian contact, this force is then convoluted with the plate's impulse response. From this, the radiated sound field is calculated by the Rayleigh integral in the time domain. In a following step, an active force is used to act on the plate with the purpose of minimizing the radiated sound power. This control force is estimated using a method based on the LMS algorithm formulated in the time-domain. For different positions of the impact between the sphere and the plate, the position of the active force is varied and for each case, the LMS algorithm obtains the optimal time record of the force. For non-trivial cases, where the acting force is not in the same position as the impact, results present reductions of up to 13 dB in the simulations of the radiated sound power.

Keywords: Active noise control, Impacts I-INCE Classification of Subjects Numbers: 38.3, 41.3

1. INTRODUCTION

Whether in residences or in the workplace, impacts are an important source of noise in today's society. The concern with this type of noise increases in industry due to the large presence of machinery whose mechanical processes include impacts (1) Planing, pressing, stamping, forging and other hammer-type operations are some examples of such machines. Because of the materials involved, the sound pressure levels resulting from these impacts can present a health risk, leading to a need of legislation (2). However, given the transient nature and short duration of impact noise, the produced sound is difficult to control, culminating in a larger struggle to meet the emission regulations (3).

With the use of passive absorbers, it is possible to attenuate high frequencies in the radiated sound resulting from the impacts. Nonetheless, this might lead to an obstruction of the access to the machine. Another concern with this type of solution is the impractical control of lower frequencies and vibrations. Thus, for an effective result, actions must be taken at the source level. When dealing with impacts, this source level is the contact between the colliding bodies, meaning that by controlling the way this collision occurs, it is possible to control all the subsequent outcomes of the impact. For this, active control can be of great value.

The concept of active control applied in this research is the use of electroacoustic transducers to modify/control sound fields. To simplify this rather broad topic, a sphere impacting on a plate which is simply supported by an infinite baffle was selected as the generic study case. An artificial active force applied to the plate is the chosen actuation method. The aim of this paper is to investigate possible active control measures with the purpose of reducing the radiated sound resulting from such an impact. To determine the control measures, a time-based Least Mean Square (LMS) algorithm is used to estimate the optimal active force to be applied to the plate in order to reduce the radiated sound.

Although this setup does not cover many of the features present in the aforementioned industrial machinery, it is considered sufficient as a theoretical setup to be used as a first step for more complex constructions. This is a necessary provision, given that there is a rather small amount of literature on the use of active control for impact problems, especially from an acoustic point of view.

This paper is organized in the following way: Section 2 contains the pertinent theoretical background used in this work. Section 3 presents the setup used to explore the presented problem by

[1] pandre@student.chalmers.se
[2] wolfgang.kropp@chalmers.se

means of a numerical study using a case of uncorrelated acting and contact force. Section 4 presents further discussion on the results of the numerical study. Lastly, section 5 concludes the work with final remarks on possible future studies.

2. THEORETICAL BACKGROUND

The concept behind the method used in this work is the application of the LMS-algorithm to estimate the optimal control force to minimize the radiated sound power resulting from an impact. Thus, this section is subdivided in two parts. First, a presentation on the theoretical formulations to estimate the impact force and the resulting radiated sound is presented. Second, a brief description of the LMS-algorithm as well as how this algorithm can be used for optimal force estimation is demonstrated.

2.1 Radiated sound power of an impact

An impact process has been shown to include several sub-mechanisms that generate sound and/vibrations (2). This paper focuses solely on the radiated sound due to structural vibrations resulting from the impact. This is the so-called ringing noise. To calculate this noise, the theoretical formulation presented in (1) was used, where three successive calculations are required:

- first the impact force must be estimated;
- second the response of the plate to an impulsive force is determined;
- third the acoustic pressure at a specific given point is found.

2.1.1 Impact force

To describe the impact force, a nonlinear relation to the sphere's displacement was used. This nonlinear relation is given by Hertz's law and is written as

$$F_I = s \cdot u(t)^{3/2} \tag{1}$$

Where $u(t)$ is the sphere's displacement relative to the plate or the sphere's deformation, F_I is the impact force and s is Hertz's constant, which is a parameter of both the sphere and plate material and found through

$$s = \frac{4}{3}\sqrt{R} \cdot \left[\frac{1-\nu_1^2}{E_1} + \frac{1-\nu_2^2}{E_2} \right]^{-1} \tag{2}$$

Where R is the radius of the sphere, E_1 and E_2 are the Young's modulus of the sphere and plate and ν_1 and ν_2 the respective Poisson's ratios. There are three necessary assumptions for the use of this relation. The first assumption is that the strains are small and within the elastic limit. The second is that the surfaces are frictionless. The third is that the area of contact is much smaller than the objects involved in the impact.

The equation of motion of the sphere is thus necessary to find the displacement present in equation 1. Applying Newton's second law, the following is obtained

$$m_s \cdot \frac{d^2}{dt^2}\big(u(t) + w(t)\big) = F_I \tag{3}$$

Where m_s is the mass of the sphere and $w(t)$ is the displacement of the plate at the contact point. Hence, the expression $u(t)+w(t)$ represents the absolute displacement of the sphere. The last step needed to find the impact force is to find the displacement of the contact point of the plate. This is found with the plate's impulse response, given by

$$w(t) = \int_0^t F_I(t) \cdot M(t-\tau)\, d\tau \tag{4}$$

Where M is the impulse response of the plate. This is a very similar response to the one that will be needed in the next step of calculations, as mentioned previously, and is expressed by

$$M(t) = -\frac{4}{m_p} \sum_{n=1}^{\infty} \sum_{m=1}^{\infty} {\Phi^2}_{n,m,c} \frac{\sin\left(\theta_{n,m} t\right)}{\theta_{n,m}} e^{-\delta_{n,m} t} \tag{5}$$

Where m_p is the mass of the plate, $\Phi_{n,m,c}$ is the plate's eigenfunction at the contact point (x_c,y_c), and $\theta_{n,m}$ and $\delta_{n,m}$ are values related to the eigenfrequencies which are expressed by

$$\theta_{n,m} = \omega_{n,m}\sqrt{1-\frac{\eta^2}{4}} \tag{6.a}$$

$$\delta_{n,m} = \frac{\eta}{2}\omega_{n,m} \tag{6.b}$$

Where $\omega_{n,m}$ are the eigenfrequencies, which for a rectangular plate are found by

$$\omega_{n,m} = \sqrt{\frac{B}{m''}}\cdot\left[\left(\frac{n\pi}{L_x}\right)^2+\left(\frac{m\pi}{L_y}\right)^2\right] \tag{7}$$

Where L_x and L_y are the length and width of the plate, $m''=\rho_p h$ is the mass per unit area of the plate, B is the bending stiffness of the plate.

For the case studied, which evaluates a simply supported plate, the eigenfunctions are expressed as

$$\Phi_{n,m,c} = \sin\left(\frac{n\pi\ x_c}{L_x}\right)\sin\left(\frac{n\pi\ y_c}{L_y}\right) \tag{8}$$

With equations 1 through 8, it is possible to create a function that describes the relative displacement of the sphere as a function of time. This function can be solved numerically with the use of the Newton-Rhapson method, with the initial step using the velocity of the sphere after a free fall, and the Hilber-Hughes-Taylor Method, used to relate the time derivatives described in the equations above.

Besides the contact force, a viscous damping force was added to model losses and introduce damping in the system. This force is proportional to the sphere's velocity relative to that of the plate and is modelled as:

$$F_v = c(t)\cdot\dot{u}(t) \tag{9}$$

Where c is the viscous damping factor, defined as time dependent to avoid discontinuities and proportional to $u(t)$.

2.1.2 Plate impulse response to an impulsive force

The next step is the calculation of the plate's impulse response to an impulse. The only necessary modification to equation 5 is that now the receiving position is not the same as the contact point. Thus, the equation becomes

$$M(x_p,y_p,t) = -\frac{4}{m_p}\sum_{n=1}^{\infty}\sum_{m=1}^{\infty}\Phi_{n,m,c}\Phi_{n,m,p}\frac{\sin\left(\theta_{n,m}t\right)}{\theta_{n,m}}e^{-\delta_{n,m}t} \tag{10}$$

Where (x_p,y_p) is a point within the plate and $\Phi_{n,m,p}$ is expressed as in equation 8 but for the coordinates with the subscript p.

2.1.3 Sound pressure at a specific point

The final step in the calculations is the calculation of the acoustic pressure at a specific point. This is done through the numerical evaluation of the Rayleigh integral, which is given by

$$p(x_r,y_r,t) = \frac{\rho_0}{2\pi}\int_S\frac{\ddot{w}(x_p,y_p,t)}{R_r}dS \tag{11}$$

Where ρ_0 is the air density, $\ddot{w}$ is the acceleration of point (x_p,y_p) in the plate and R_r is the distance between this point and the receiving point. The acceleration of the points in the plate can be estimated using a convolution between the forces applied to the plate and the second derivative in terms of time of the impulse response described in section 2.1.2.

2.2 Finding the optimal acting force

To find the optimal acting force to reduce the radiated sound from the plate, a time-domain formulation of the Least Mean Square (LMS) algorithm was applied.

2.2.1 Introduction to the LMS algorithm

The LMS algorithm is a tool used in filter design that relies on an iterative process to find the optimal filter coefficients that minimize a predetermined error function (4), as illustrated in figure 1.

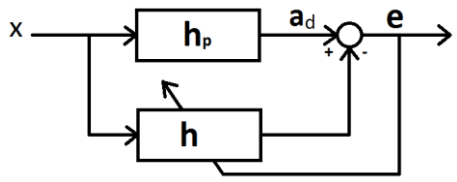

Figure 1 – Block diagram of the LMS-algorithm.

The fundamental concept behind the LMS algorithm is to update the filter coefficients by amounts proportional to the steepest gradient of the mean square error, hence the algorithm's name, at the current time step. The error used in the algorithm is the difference between the output of the system, also called desired signal, and the output of the designed finite impulse response (FIR) filter, which is expressed as:

$$e(n) = a_d(n) - \sum_{i=1}^{I} x(n-i) \cdot h(i) \tag{12}$$

Where $e(n)$ is the error at the time step n, a_d is the desired signal at this time step which is the value that the filter should try to mimic, x is the input signal observed, h is the filter coefficients and I is the length of the filter, which is the length of the FIR filter. The sum in equation 12 is the convolution between the input signal until the current time step and the designed filter, which in vector form is represented as:

$$e(n) = a_d(n) - \mathbf{h}^T(n)\,\mathbf{x}(n) \tag{13}$$

Where T indicated the transpose of the vector, which are

$$\mathbf{h}^T(n) = \left[h_1(n), h_2(n), ..., h_I(n)\right] \tag{14.a}$$

$$\mathbf{x}^T(n) = \left[x(n), x(n-1), ..., x(n-I)\right] \tag{14.b}$$

With the error function defined, it is thus necessary to find the filter coefficients that minimize this function. As mentioned before, the LMS algorithm uses the mean square error as a criterion for this. Thus the cost function for this algorithm is expressed as:

$$C(n) = E\left[e^2(n)\right] = E\left[\left(a_d(n) - \mathbf{h}^T(n)\,\mathbf{x}(n)\right)^2\right] \tag{15}$$

Where C is the cost function, $E[e^2(n)]$ is the expected value of the error. This leads to the analysis that the cost function is a quadratic equation in terms of result from the convolution of the filter coefficients and the input signal. Hence, the concept of the steepest decline of the filter coefficients can be followed to reach the global minimum of the function. One can express the concept of steepest decline through the gradient of the cost function:

$$\nabla \cdot C(n) = \frac{\partial E\left[e^2(n)\right]}{\partial h_i} = 2E\left[e(n)\frac{\partial e(n)}{\partial h_i}\right] = -2E\left[e(n)x(n-i)\right] \tag{16}$$

This gradient allows for the formulation of the iterative method to find the optimal filter coefficients, which is written as:

$$\mathbf{h}(n+1) = \mathbf{h}(n) - \alpha \nabla C(n) = \mathbf{h}(n) - 2\alpha E\left[e(n)x(n-i)\right] \tag{17}$$

Where α is a weighting factor that determines the step size of the process. The expected value of the error often must be estimated. This estimation can be done using the instantaneous value of the

gradient for the current time step. This will adjust the filter coefficients in a way to minimize the mean square error on average. Equation 17 thus becomes:

$$\mathbf{h}(n+1) = \mathbf{h}(n) - \alpha e(n)\mathbf{x}(n) \tag{18}$$

With the method defined, it is necessary to find the appropriate step size for the process. This step size influences both the time the algorithm needs to reach the optimal solution as well as the convergence of the algorithm. This influence is that the smaller the step is, the better the convergence and the longer the time necessary for the solution to be reached. To guarantee convergence, the value of α must fulfill the following expression:

$$0 \leq \alpha \leq \frac{1}{I \cdot E\left[x^2(n)\right]} \tag{19}$$

This algorithm presents a rather low sensitivity to noise due to the use of the average gradient. Hence, if the noise is affecting the instantaneous time step, the average will still lead towards the global minimum, only requiring a longer time to reach it.

2.2.2 Adaptations to the LMS algorithm

The application of the LMS algorithm in this work is to identify the optimal control force to be applied on a specific position of the plate. This means that the filter coefficients can be found by means of the theoretical formulations presented in equation 20, and thus, the input to the system can be changed to be the desired result. Upon evaluation of the derivation of the LMS algorithm, one notices the need to change only the step where the gradient is calculated in order to obtain the expression that will find the optimal input instead of filter coefficients. Expression 16 thus becomes:

$$\nabla \cdot C(n) = \frac{\partial E\left[e^2(n)\right]}{\partial x_i} = 2E\left[e(n)\frac{\partial e(n)}{\partial x_i} \right] = -2E\left[e(n)h(i)\right] \tag{20}$$

Leading to the following formulation of the iterative process:

$$\mathbf{x}(n+1) = \mathbf{x}(n) - 2\alpha E\left[e(n)h(i)\right] \tag{21}$$

Now however, a problem with the expected value arises. Previously, the quadratic error would reach the desired level of reduction if the input signal was sufficiently long to obtain a good enough average of the expected value. In the new situation presented in this section, the input is cut off and each unknown input value, $\mathbf{x}(n)$ will only be updated I times due to the length used for the FIR filter. This limited amount of updates might not be sufficient to reach the desired optimum point. A trick, presented in (4) that can be applied to solve this problem is to use only a part of the input signal, with the length N, and periodically repeat the filter coefficients with a period length of N as well as the desired signal. This will create an analogy to the standard LMS algorithm, permitting the analogical description of the iterative process as:

$$\mathbf{x}(n+1) = \mathbf{x}(n) - \alpha e(n)\mathbf{h}(n) \tag{22}$$

The length used for the input value must be, in practice, at least twice that of the filter length I. This is because the first I values of the desired signal are also influenced by values outside of the observation window (which has the length of N).

Next, since the LMS algorithm will be applied to find the optimal force to reduce the radiated sound of the plate, the system should not be analyzed only for one receiving position but for many points around the plate that can sufficiently recreate the sound power from the plate. For each receiving position, there is a specific impulse response which represents one input to the LMS algorithm. The LMS algorithm presented previously is limited to one input and thus needs to be generalized in order to function for multiple inputs. To do this, it is first necessary to specify the error for each receiving position:

$$e_r(n) = a_{dr}(n) - \sum_{s=1}^{S} \mathbf{h}_{sr}^T(n)\, \mathbf{x}_\mathbf{s}(n) \tag{23}$$

The subscript r indicates a specific receiving position, the subscript s indicates an excitation force, therefore $\mathbf{h}_{sr}(n)$ represents the impulse response for a specific excitation force and receiving position at the current time step, and S is the total amount of excitation forces. The error in equation 23 is then used to update the force coefficients. However, given that there are multiple forces, an average of the

gradient is performed to find the average optimal direction towards the minimum. The process is then formulated as:

$$\mathbf{x}(n+1) = \mathbf{x}(n) - \langle \alpha_r e_r(n) \mathbf{h}_{\mathbf{sr}}(n) \rangle \tag{24}$$

The < > symbol represents the average over the receiving positions. It is important to emphasize that the current time step n must be larger than the FIR filter length. One last consideration is the limit of the weighting factor α, which due to the increase in degrees of freedom, must be defined with more restriction. The following relation expresses this:

$$0 \leq \alpha \leq \left(\frac{N}{R} \sum_{r=1}^{R} \sum_{i=0}^{I} |\mathbf{h}_{\mathbf{sr}}(i)|^2 \right)^{-1} \tag{25}$$

Where N is the length of the input signal and R is the number of receiving positions. The final diagram that represents this adapted LMS-algorithm is illustrated in figure 2.

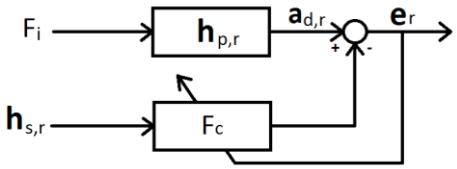

Figure 2 – Block diagram of the LMS algorithm used in this work.

3. SETUP AND RESULTS

Here the setup adopted as well as the result for each step in the used methodology is shown. In section 3.1 the studied case and parameters used are fully described. Section 3.2 shows the obtained contact force for different impact locations within the plate as well examples of the transfer functions obtained. Section 3.3 shows the acting force obtained from the LMS algorithm.

3.1 Simulation setup

The simply supported plate selected for the simulations performed in this study is made of Plexiglas, with a length of 0.8 m, a width of 0.7 m and a thickness of 0.035 m. The sphere chosen is a made of steel with a radius of 0.02 m. The detailed material properties used in the calculations are presented in table 1.

Table 1 – Overview of material properties used

Material	Plexiglas	Steel
Density, kg/m³	1150	7800
Elastic Modulus, N/m²	$5.6 \cdot 10^9$	$210 \cdot 10^9$
Poisson's ratio	0,3	0,31
Loss factor	0,02	-
Viscous damping	12	-

The main reason for the choices presented above were simplicity and availability of the evaluated specimens. Both steel and Plexiglas are largely available and used in today's industry.

For the initial conditions in the studied case, the sphere was dropped at a height of 5 cm from the plate surface, with no initial velocity. The plate is initially at rest and has it's top surface at the xy-plane of the used coordinate system. The point of impact between sphere and plate as well as the point where the control force is applied were varied in order to study control effort and effectiveness of the proposed control method. The receiving half-sphere selected for this work has a 10 m radius with 513 receiving positions in it. This is to guarantee that assumptions relying on far-field pressure are satisfied.

A value of α_{HHT} = -1/3 was used for the HHT algorithm. In all simulations, the gravitational

constant of g = -9.81 m/s², the speed of sound c_0 = 340 m/s and the air density ρ_0 = 1.2 kg/m³ were used. Lastly, a time step of size $\Delta t = 1 \cdot 10^{-6}$ s was defined in order to properly represent an impact, given its short duration.

The determination of the time step size, implies the definition of the frequency limit used in this work as well. Thus, the impulse responses calculated using the equations presented in chapter 2 have an upper limit in the mode summation. This limit is determined by a limit to the eigenfrequency of the modes, expressed by $\omega_{n,m,max} = \pi/\Delta t$.

3.2 Impact force and transfer functions

Three example impact locations were chosen for the simulation. These are described in table 2 and illustrated in figure 3.

Table 2 – Example impact locations

Position	Coordinate
Impact Position 1	(0,4; 0,35)
Impact Position 2	(0,6; 0,6)
Impact Position 3	(0,3; 0,15)

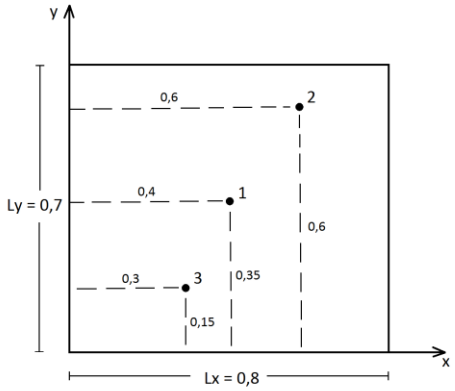

Figure 3 – Sketch of the simply supported plate and some impact positions simulated

With the setup described in the previous section and the impact locations determined, it was possible to calculate the impact forces for each position. The obtained forces are shown in figure 4.

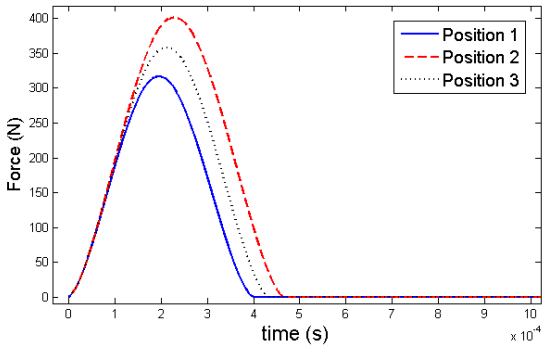

Figure 4 – Impact forces for different impact positions

The dependency of the impact force in relation to position, shown in figure 4, is as expected. Where the closer the impact is to an edge, the higher the force will be due to a higher stiffness in the borders of the plate. The duration of the impact as well as the shape of the force is also consistent with what is found in works such as (2).

The next step in the calculations is the computation of the transfer function between the acoustic pressure at a certain point and a force applied at a certain position in the plate. For this, the frequency limit presented in section 3.1 must be also applied to the discretization of the plate, which is used in the

Rayleigh integral. However, the time step used now does not need to be so small. Since a smaller step implies in a much larger computational effort and also much more frequency information than what is of interest, the time step was altered to resolve these issues. Thus, for the definition of the time step, an analysis of the radiation efficiency of the plate was performed. Figure 5 shows the radiation efficiency for the studied plate as well as for its first 15 modes.

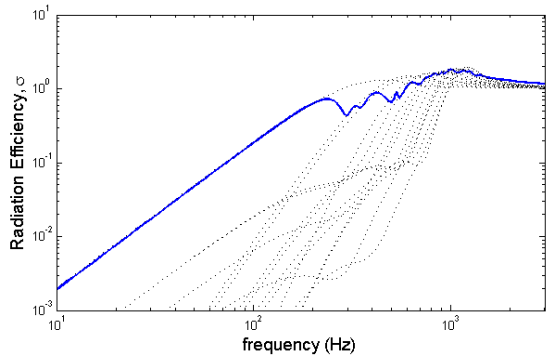

Figure 5 – Radiation efficiency of the studied plate. The solid blue line represents the efficiency achieved from modal superposition and the dotted black lines are the efficiencies of the first 15 modes separately.

From figure 5 it is possible to determine the coincidence frequency of the plate, which is around 1 kHz. In addition, the impact force acts as a low pass filter, having a cutoff frequency of around 3 kHz. Thus, the frequency range of interest chosen was from 0-2,5 kHz, which determines the necessary sampling frequency to be at least 5 kHz, and therefore, the time step becomes $\Delta t = 2 \cdot 10^{-4}$ s.

With the frequency range determined, the discretization of the plate for the Rayleigh integral could also be derived. A rule of thumb of the finite element method states that at least six elements are necessary to properly represent a certain wavelength. Taking the eigenfrequency of highest mode evaluated, with respect to this new time step and the speed of sound for bending waves, the smallest evaluated wavelength is obtained. For the case studied, this lead to a discretization of the plate by a step size of $\Delta x = \Delta y = 0{,}0125$ m.

The half-sphere used in this work is represented by 513 uniformly distributed discrete points, which means that 513 receiving positions are used to estimate the radiated sound power from the plate. This half-sphere has a 10 m radius to guarantee that the assumption of far field pressure is valid. Hence, there are 513 transfer functions that must be calculated and evaluated in the simulations. One example of these is shown in figure 6.

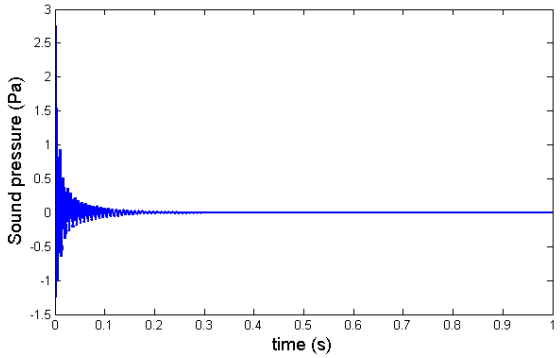

Figure 6 – Example of transfer function between the acoustic pressure and an impulsive force at a receiving point 10 m away from the plate.

Next, the impact force must be resampled to have the same time step as the transfer function. With this, it is possible to convolute both the transfer function and the impact force to find the desired signal, which will be used in the LMS-algorithm. Again, there will be 513 of convolutions with the changes described in section 2.2.2, the LMS-algorithm will attempt to reduce the error between these desired signals and the signal from the acting force by means of an average of the errors. Figure 7 shows an example of these desired signals.

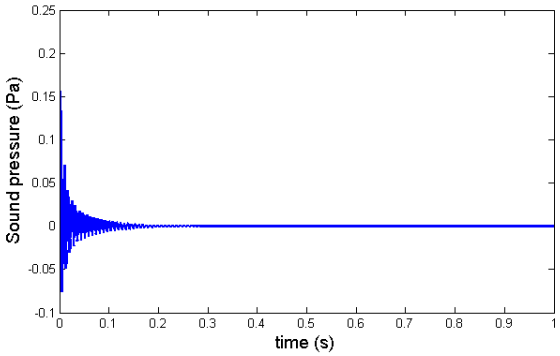

Figure 7 – Example of desired signal used in the LMS-algorithm.

3.3 LMS-algorithm

For each impact position, four different acting force positions were tested including the trivial case of the acting force acting on the point of impact. Table 3 presents the coordinates of the chosen control force positions.

Table 3 – Control force application locations

Position	Coordinate
Control Position 1	(0,4; 0,35)
Control Position 2	(0,6; 0,6)
Control Position 3	(0,3; 0,15)
Control Position 4	(0,4; 0,6)

As described in section 2.2.2, the LMS-algorithm is repeated in many iterations with the intention of improving the estimations of the optimal acting force through the updating of its value several times. For the simulations performed in this work, 100 iterations were considered enough. In figures 8 through 10 are the results for the obtained acting force and the relative error between iterations for each of the evaluated positions. This relative error is considered for each of the 513 receiving positions, and thus, the graphs illustrating it have a line for each position. However, only the general trend of this graph is of interest, so no detailed view of each line is necessary.

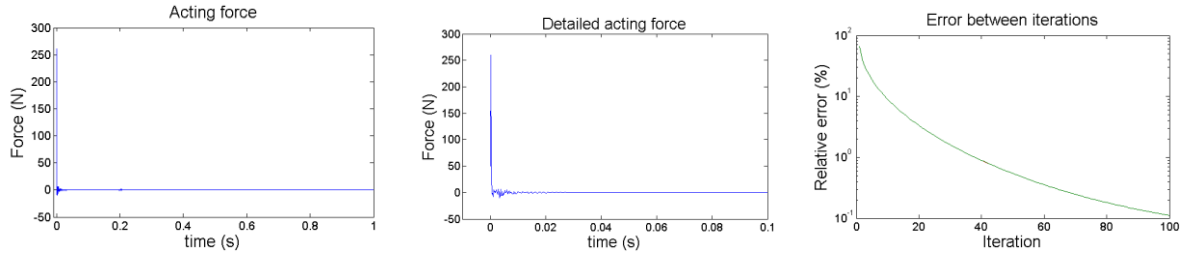

a) Control Position 1

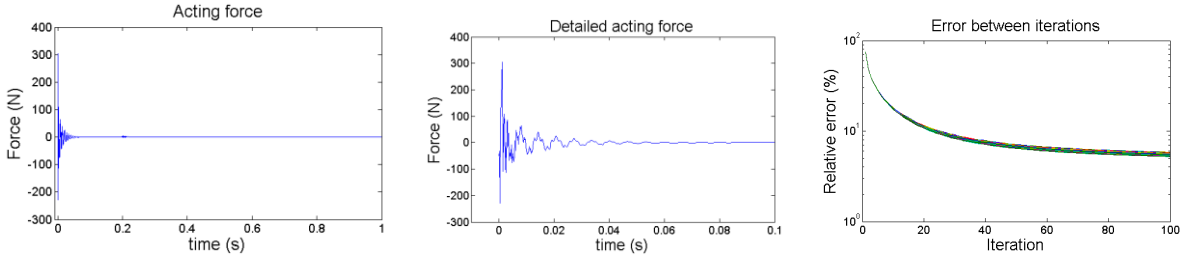

b) Control Position 2

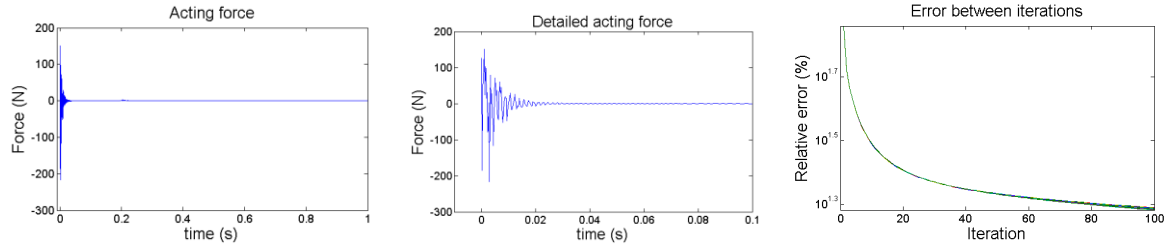

c) Control Position 3

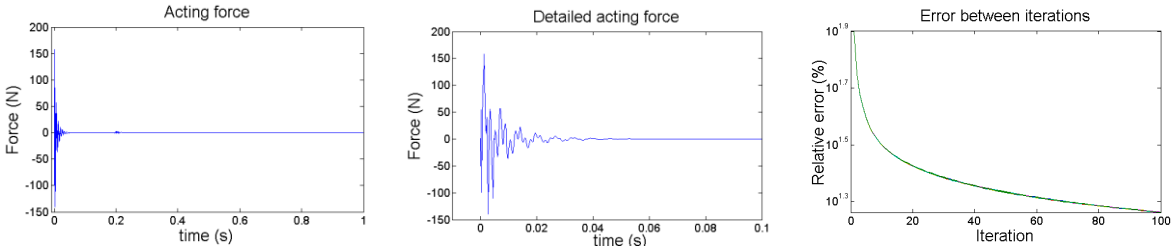

d) Control Position 4

Figure 8 – Acting forces obtained at different control positions for impact position 1. On the left, the full acting force is shown, in the center a more detailed view of this force is presented and on the right the error between iterations to reach this force is illustrated.

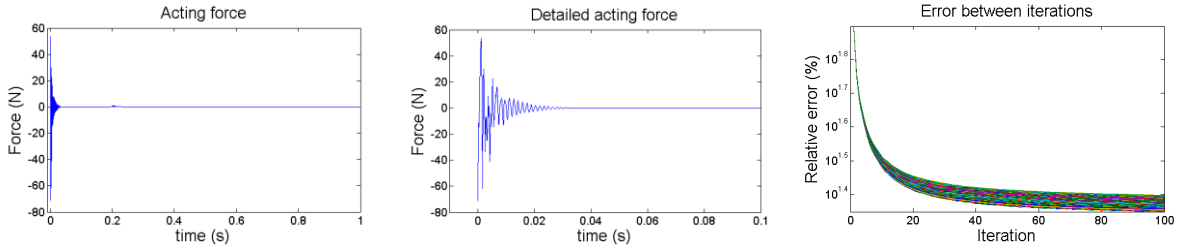

a) Control Position 1

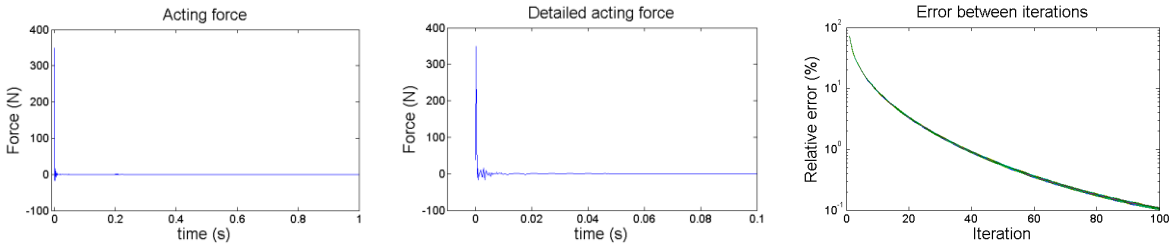

b) Control Position 2

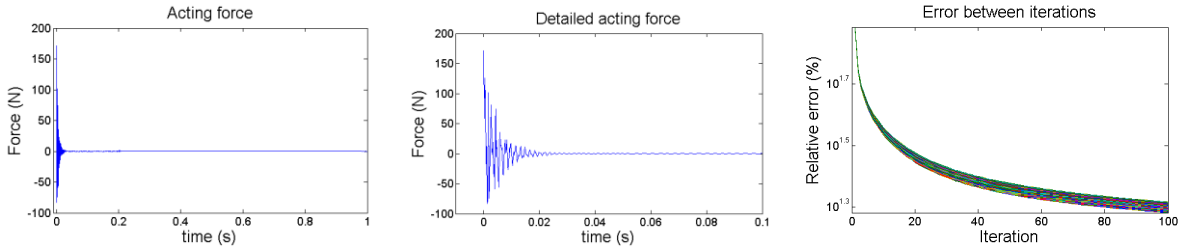

c) Control Position 3

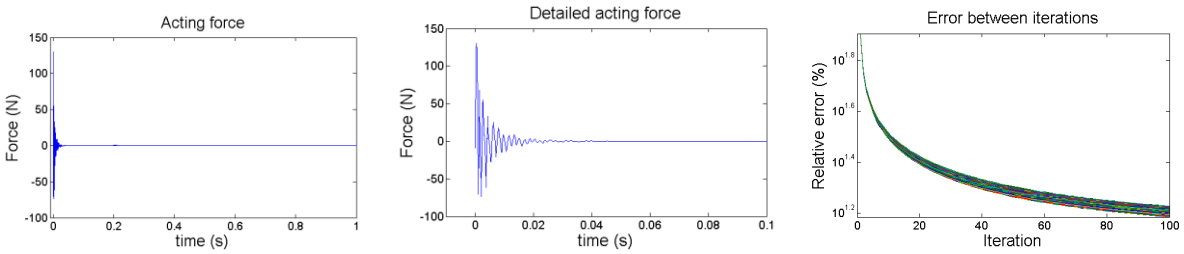

d) Control Position 4

Figure 9 – Acting forces obtained at different control positions for impact position 2. The layout is similar to figure 8.

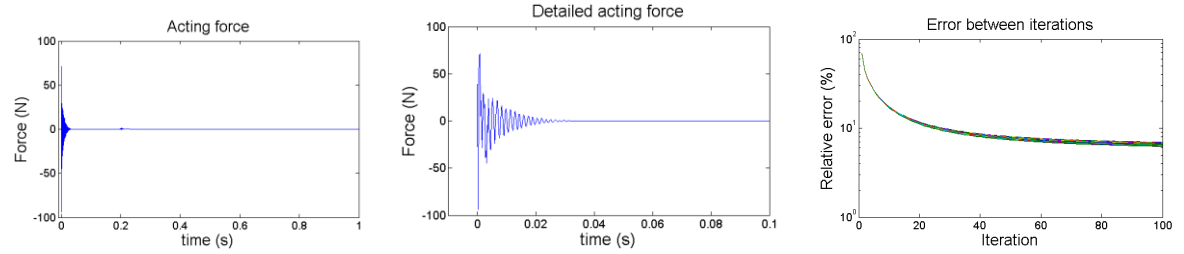

a) Control Position 1

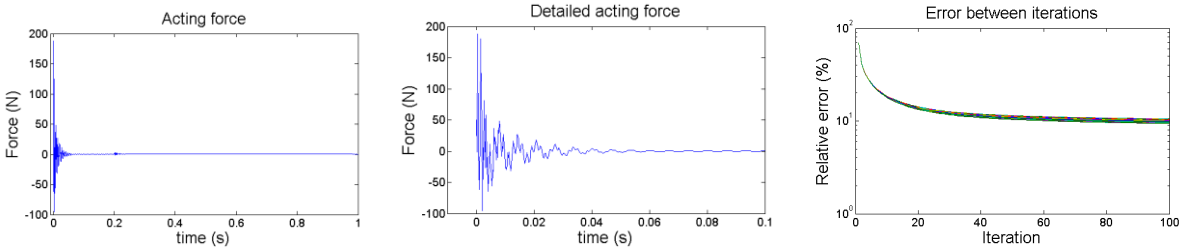

b) Control Position 2

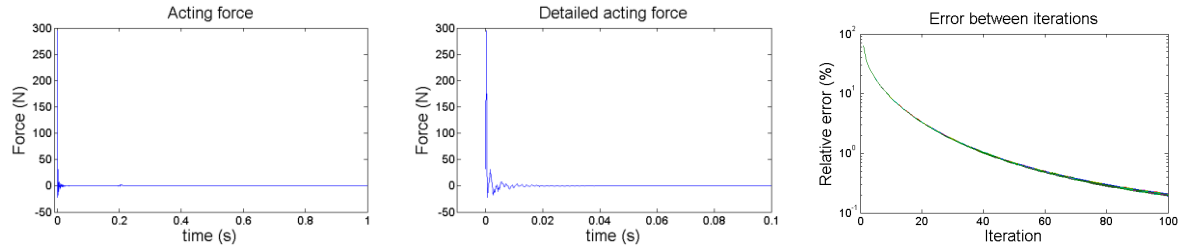

c) Control Position 3

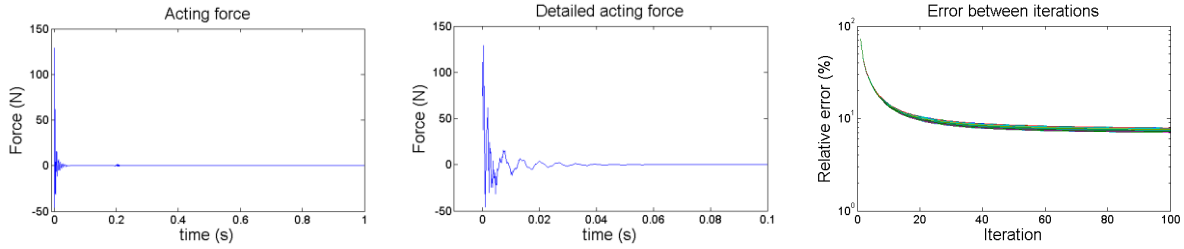

d) Control Position 4

Figure 10 – Acting forces obtained at different control positions for impact position 3. The layout is similar to figure 8.

From figures 8 to 10 it is easy to note that the obtained acting forces mimic the impact force to a certain extent. This is especially true for the cases where the forces are applied in the same position, where the optimal acting force is known to be the exact replica of the contact force. Comparing these cases with figure 4, it is possible to verify that the LMS-algorithm is working as desired.

Lastly, the total radiated sound power was calculated by summing up the sound intensities over the half sphere of receiving positions. This sound power was compared to a situation with and without the acting force to measure the resulting reduction. Table 4 presents the achieved reduction for each impact position and acting force position pair.

Table 4 – Reduction for each impact force and acting force position pair.

	Control Position 1	Control Position 2	Control Position 3	Control Position 4
Impact Position 1	-31,1 dB	**-12,9 dB**	-7,3 dB	-7,6 dB
Impact Position 2	-6,4 dB	-30,3 dB	-7,2 dB	**-8,1 dB**
Impact Position 3	-8,4 dB	-10,3 dB	-27,9 dB	**-11,5 dB**

From table 4 it is possible to extract that there is no optimal position for the application of the control force. However, when considering the symmetry of the studied plate, one finds that the highest reductions arise from cases where the acting force is applied closest to the impact position, excluding the trivial positions. One case that deserves a deeper evaluation is presented in figure 10, where cases b and d are equidistant from the impact force. The reason for the higher reduction in control position 4 is that this position is less stiff than control position 2 and thus requires a smaller control effort as well. This is a rather expected result, but the realization that the acting force can be position in a strategic position with consideration to symmetry is very important.

4. FINAL REMARKS

The formulation of the time domain LMS algorithm used in this work successfully resulted in acting forces which lowered the sound power radiated from a simply supported plate impacted by a sphere. For all cases evaluated in this work, reduction in the resulting sound power was achieved. Therefore, there is a strong indication that impact control by means of an external control force applied to the impacted structure is possible.

For cases where the acting force is applied to the point where the impact occurs, reductions of up to 30 dB were obtained. For positions other than that, the obtained reduction in sound power varied from 6 to 12 dB. Results from the cases studied in this work show that the closer the impact and acting positions are, the higher the reduction will be with a smaller necessary control effort as well. This observation also applies to cases where symmetry in the impacted structure exists, which was the case studied in this paper.

Suggestions of further work is the development of an experiment to verify the applicability of the method proposed here, as well as an analysis on the coupling between experimental results and simulated ones.

ACKNOWLEDGEMENTS

The authors would like to acknowledge the help of Carsten Hoever and Lars Hansson in the development of this work. This work has been produced during the first author's scholarship period at Chalmers University of Technology, thanks to a Swedish Institute scholarship.

REFERENCES

1. Troccaz P, Woodcock R, Laville F. Acoustic radiation due to the inelastic impact of a sphere on a rectangular plate. J Acoust Soc Am, 2000;108(5):2197–2202.
2. Hoever C. Active structural control of impacts with a view towards noise control. Technische Universität Berlin; 2008.
3. Micallef C. Active control of impact noise. Chalmers University of Technology; 2003.
4. Kropp W, Larsson K. Force estimation in the time domain by applying an LMS algorithm. Proc NOVEM 05; 18 April 2005; Saint-Raphaël, France 2005.
5. Amiryarahmadi N, Kropp W, Larsson K. Application of LMS algorithm to measure low-frequency transient forces from human walking. Acta Acoustica united with Acustica. 2016;102(1):23-34.